Dussertite $BaFe^{3+}_3(AsO_4)_2(OH)_5$ – A Raman spectroscopic study of a hydroxy-arsenate mineral

Ray L. Frost, [1] • Silmarilly Bahfenne, [1] Jiří Čejka, [1,2] Jiří Sejkora,[2.] Jakub Plášil, [2] Sara J. Palmer [1], Eloise C. Keeffe [1], Ivan Němec [3]

[1] Inorganic Materials Research Program, School of Physical and Chemical Sciences, Queensland University of Technology, GPO Box 2434, Brisbane Queensland 4001, Australia.

[2] National Museum, Václavské náměstí 68, CZ-115 79 Praha 1, Czech Republic.

[3] Department of Inorganic Chemistry, Charles University in Prague, Faculty of Science, Hlavova 8, CZ-128 43, Praha 2, Czech Republic

The mineral dussertite, a hydroxy-arsenate mineral of formula $BaFe^{3+}_3(AsO_4)_2(OH)_5$, has been studied by Raman complimented with infrared spectroscopy. The spectra of three minerals from different origins were investigated and proved quite similar, although some minor differences were observed. In the Raman spectra of Czech dussertite, four bands are observed in the 800 to 950 cm^{-1} region. The bands are assigned as follows: the band at 902 cm^{-1} is assigned to the $(AsO_4)^{3-}$ ν_3 antisymmetric stretching mode, at 870 cm^{-1} to the $(AsO_4)^{3-}$ ν_1 symmetric stretching mode, and both at 859 cm^{-1} and 825 cm^{-1} to the As-O$M^{2+/3+}$ stretching modes/and or hydroxyls bending modes. Raman bands at 372 and 409 cm^{-1} are attributed to the ν_2 $(AsO_4)^{3-}$ bending mode and the two bands at 429 and 474 cm^{-1} are assigned to the ν_4 $(AsO_4)^{3-}$ bending mode. An intense band at 3446 cm^{-1} in the infrared spectrum and a complex set of bands centred upon 3453 cm^{-1} in the Raman spectrum are attributed to the stretching vibrations of the hydrogen bonded $(OH)^-$ units and/or water units in the mineral structure. The broad infrared band at 3223 cm^{-1} is assigned to the vibrations of hydrogen bonded water molecules. Raman spectroscopy identified Raman bands attributable to $(AsO_4)^{3-}$ and $(AsO_3OH)^{2-}$ units.

• Author to whom correspondence should be addressed (r.frost@qut.edu.au)

KEYWORDS: dussertite, arsenate, crandallite group, Raman spectroscopy, infrared spectroscopy, hydroxyl ions, molecular water, adsorbed water

INTRODUCTION

Dussertite is a rare member of the crandallite group, which belongs to a large family of isostructural compounds having the general formula $AB_3(XO_4)(OH, H_2O)_6$, where A = M^+, M^{2+}, M^{3+} and/or M^{4+} cations, B = M^{3+} (and minor M^{2+} cations, such as Cu^{2+}, Zn^{2+} and M^{5+}, such as Nb^{5+} and Ta^{5+}), and X = P^{5+}, As^{5+}, S^{6+}, Cr^{6+} and minor Si^{4+} [1]. There are some discrepancies in its chemical formula reported in the literature $BaFe^{3+}{}_3(AsO_4)_2(OH)_5$ [2], $BaFe_3(AsO_4)_2(OH, H_2O)_6$ [1, 3]. Walenta ascribed to dussertite the chemical formula $BaFe_3H(AsO_4)_2(OH)_6$ [4] and later $BaFe_3(AsO_4)_2(OH)_5.H_2O$ [5]. This agrees with the formula published by Winchell and Winchell [6] and Fleischer *et al.* [7]. Thus, the question if dussertite contains molecular water in its structure remains open. The mineral dussertite is formed through the alteration of arsenopyrite [2] or other As-containing primary minerals under oxidising conditions. Kolitsch *et al.* [1, 8] described the structure of antimonian dussertite, in which was inferred the substitution of Sb^{5+} for Fe^{3+} and not for As^{5+}. The space group of trigonal dussertite is *R*-3*m* and the unit-cell parameters are a = 7.4244(3) and c = 17.494(1) Å, Z= 3. The crystal structure is of the alunite-type and consists of sheets of corner-sharing $(Fe^{3+},Sb^{5+})O_6$ octahedra parallel to (0001). The icosahedrally coordinated Ba^{2+} cations occupy cavities between pairs of octahedral sheets and are surrounded by six oxygen atoms from the $(Fe^{3+}, Sb^{5+})O_6$ octahedra. The possible presence of $(AsO_3OH)^{2-}$ in the crystal structure of antimonian dussertite was not inferred from the structure analysis . On the contrary, in the refined crystal structure of analogous phosphate - gorceixite, the presence of $(PO_3OH)^{2-}$ groups was inferred in the disordered tetrahedral position of its crystal structure.

The aim of this paper is to report the Raman spectra of dussertite, and to relate the spectra to the molecular and crystal chemistry of this arsenate type mineral. The paper follows the systematic research on Raman and infrared spectroscopy of secondary minerals containing oxy-anions formed in the oxidation zone [9-21].

EXPERIMENTAL

Minerals

The studied sample of the mineral dussertite was found at the open pit at Huber-stock deposit, Krásno near Horní Slavkov, Horní Slavkov ore district, the Slavkovský les

Mountains, western Bohemia, Czech Republic, and is deposited in the mineralogical collections of the National Museum, Prague. The sample was analysed for phase purity by X-ray powder diffraction. No minor significant impurities were found. Its refined unit-cell parameters for trigonal space group *R*-3*m*, *a* 7.3875(5), *c* 17.484(1) Å, *V* 826.4(1) Å^3 [22], are comparable with the data published for this mineral phase [1, 22].

The dussertite sample was quantitatively analysed by Cameca SX100 microprobe system in wavelength dispersion mode for chemical composition. Studied sample was mounted into the epoxide resin and polished. The polished surface was coated with carbon layer 250 Å. An accelerating voltage of 15 kV, a specimen current of 10 nA, and a beam diameter of 5 - 10 μm were used. The following lines and standards were used: Kα: andradite (Ca, Fe), InAs (As), sanidine (Al, Si), fluorapatite (P), ZnO (Zn), baryte (S); Lα: dioptase (Cu), $SrSO_4$ (Sr), W (W); Lβ: benitoite (Ba) and Mβ: Bi (Bi). Peak counting times (CT) were 20 s for main elements and 60 s for minor elements. CT for each background was ½ of peak time. The raw intensities were converted to the concentrations using automatic *PAP* matrix correction software package. The results (mean of 3 point analysis) are CaO 0.45, BaO 17.22, SrO 0.31, CuO 0.46, ZnO 0.42, Fe_2O_3 28.54, Al_2O_3 2.72, Bi_2O_3 0.23, SiO_2 1.65, As_2O_5 24.74, P_2O_5 1.43, SO_3 0.14, WO_3 5.92, H_2O (5.71), the sum 89.94 wt. % and empirical formula $(Ba_{0.77}Ca_{0.06}Cu_{0.04}Zn_{0.04}Sr_{0.02})_{\Sigma 0.93}(Fe_{2.46}Al_{0.37})_{\Sigma 2.83}$ $[(AsO_4)_{1.48}(PO_4)_{0.14}(SiO_4)_{0.19}(WO_4)_{0.18}(SO_4)_{0.01}]_{\Sigma 2.00}(OH)_{4.37}$. The observed charge deficit on cation sites (Ba, Fe^{3+}) may be balanced by above mentioned reduction of the number of (OH) groups or by including of $(AsO_3OH)^{2-}$ groups in the crystal structure of dussertite. This should be in agreement with the ideal formula $BaFe_3[AsO_3(O,OH)]_2(OH)_6$ analogous to gorceixite. The lower sums of analyses are caused by the porous nature of the mineral studied. Based upon the methods used for calculating the formulae of minerals as may be found in published papers [22, 23], the most suitable basis for calculating the formula of dussertite is to use the elements included in anion part of the formula - (As+P+Si+W+S) = 2.00 apfu. H_2O content was calculated on the basis of charge balance.

The Raman spectra of two dussertite minerals from Djebel Debar, Algeria and from Clara mine, Rankach Valley, Oberwolfach, Wolfach, Black Forest, Baden-Württemberg, and Germany [24] were downloaded from the RRUFF data base web site (http://rruff.info/dussertite/display=default/). The spectra were used as is and were not

105 modified in any way. The chemical analysis of the dussertite from Algeria can be found in
106 Anthony *et al.* (page 152) [2].
107
108 **Raman spectroscopy**
109
110 Crystals and single crystal samples of dussertite were placed on a polished metal
111 surface on the stage of an Olympus BHSM microscope, which is equipped with 10x, 20x, and
112 50x objectives. The microscope is part of a Renishaw 1000 Raman microscope system, which
113 also includes a monochromator, a filter system and a CCD detector (1024 pixels). The Raman
114 spectra were excited by a Spectra-Physics model 127 He-Ne laser producing highly polarised
115 light at 633 nm and collected at a nominal resolution of 2 cm^{-1} and a precision of ± 1 cm^{-1} in
116 the range between 200 and 4000 cm^{-1}. Repeated acquisition on the crystals using the highest
117 magnification (50x) were accumulated to improve the signal to noise ratio in the spectra.
118 Spectra were calibrated using the 520.5 cm^{-1} line of a silicon wafer. Previous studies by the
119 authors provide more details of the experimental technique. Alignment of all crystals in a
120 similar orientation has been attempted and achieved. However, differences in intensity may
121 be observed due to minor differences in the crystal orientation.
122
123 **Infrared spectroscopy**
124
125 Infrared spectra of dussertite sample were recorded by micro diffuse reflectance
126 method (DRIFTS) on a Nicolet Magna 760 FTIR spectrometer (range 4000-600 cm^{-1},
127 resolution 4 cm^{-1}, 128 scans, 2 level zero-filling, Happ-Genzel apodization), equipped with
128 Spectra Tech InspectIR micro FTIR accessory. Each sample of amount less than 0.050 mg
129 was mixed without using pressure with KBr. Samples were immediately recorded together
130 with the same KBr as a reference.
131
132 Spectral manipulation such as baseline correction/adjustment and smoothing were
133 performed using the Spectracalc software package GRAMS (Galactic Industries Corporation,
134 NH, USA). Band component analysis was undertaken using the Jandel 'Peakfit' software
135 package that enabled the type of fitting function to be selected and allows specific parameters
136 to be fixed or varied accordingly. Band fitting was done using a Lorentzian-Gaussian cross-
137 product function with the minimum number of component bands used for the fitting process.

The Gaussian-Lorentzian ratio was maintained at values greater than 0.7 and fitting was undertaken until reproducible results were obtained with squared correlations of r^2 greater than 0.995.

RESULTS AND DISCUSSION

The polyhedron $(AsO_4)^{3-}$ is of tetrahedral symmetry (T_d), exhibiting four fundamental vibrations: the ν_1 symmetric stretching vibration (A_1, ~ 820 cm^{-1}, Raman active), the doubly degenerate ν_2 symmetric bending vibration (E, ~350 cm^{-1}, Raman active), the triply degenerate ν_3 antisymmetric stretching vibration (F_2, ~ 900–850 cm^{-1}, Raman and infrared active) and the triply degenerate ν_4 bending vibration (F_2, ~ 400 cm^{-1}, Raman and infrared active) [25-32]. The $(AsO_4)^{3-}$ group is the only tetrahedral oxyanion of the main group elements, exhibiting $\nu_s > \nu_{as}$ [29, 33]. Protonation, metal complexation, and/or adsorption on a mineral surface should cause change in $(AsO_4)^{3-}$ symmetry from T_d to lower symmetries, such as C_{3v}, C_{2v} or C_1. This loss of degeneracy causes splitting of degenerate vibrations of $(AsO_4)^{3-}$ and the shifting of the As-OH stretching vibrations to different wavenumbers. Such chemical interactions reduce $(AsO_4)^{3-}$ tetrahedral symmetry, as mentioned above, to either C_{3v}/C_3 (corner-sharing), C_{2v}/C_2 (edge-sharing, bidentate binuclear), or C_1/C_s (corner-sharing, edge-sharing, bidentate binuclear, multidentate) [28, 29]. In association with $(AsO_4)^{3-}$ symmetry and coordination changes, the A_1 band may shift to different wavenumbers and the doubly degenerate E and triply degenerate F modes may give rise to several new A_1, B_1, and/or E vibrations. In the absence of symmetry deviations, $(AsO_3OH)^{2-}$ in C_{3v} symmetry exhibit the ν_s and ν_{as} As-O vibrations (As-O_3) and ν_{as} and ν_s As-OH vibrations [28, 29]. The increase of As-OH bond-lengths cause shift of pertinent vibrations to lower wavenumbers. Myneni et al. [28, 29] discussed only the stretching vibrations. The correct assignments are thus extremely difficult. The resolution of the As-OH bands properly is nearly impossible without deuteration of the samples [29]. Keller [34] assigned the following infrared bands observed in the compound $Na_2(AsO_3OH)\cdot 7H_2O$ at 450 and 360 cm^{-1} to the δ_{as} (ν_4) $(AsO_3OH)^{2-}$ bend (E), 580 cm^{-1} to the As-OH out-of-plane bend, 715 cm^{-1} to the ν As-OH stretch (A_1), 830 cm^{-1} to the ν_{as} $(AsO_3OH)^{2-}$ stretch (E), and 1165 cm^{-1} to the δ As-OH in-plane-bend. The Keller's suggested As-OH in-plane and out-of plane bending vibrations are comparable with similar attribution presented for δ P-OH in-plane and γ P-OH out-of-plane bending vibrations [34]. In

the Raman spectrum of $Na_2(AsO_3OH)\cdot 7H_2O$, Vansant *et al.*[31, 32] attributed observed Raman bands to the following vibrations: these at 55, 94, 116 and 155 cm^{-1} to the lattice modes; at 210 cm^{-1} to the ν (OH…O) stretch; at 315 cm^{-1} to the $(AsO_3OH)^{2-}$ rocking; at 338 cm^{-1} to the δ_s AsO_3 bend; 381 cm^{-1} to the δ_{as} $(AsO_3OH)^{2-}$ bend; at 737 cm^{-1} to the ν_s As-OH stretch (A_1); at 866 cm^{-1} to the ν_{as} $(AsO_3OH)^{2-}$ stretch (*E*). Because of relatively high content of P^{5+} (~0.14 apfu), also bands related to the $(PO_4)^{3-}$ and $(PO_3OH)^{2-}$ vibrations are expected to be observed in the Raman and infrared spectra ($(PO_4)^{3-}$: δ_s (ν_2) 410-490 cm^{-1}, δ_{as} (ν_4) 510-670 cm^{-1}, ν_1 930-990 cm^{-1}, ν_3 975-1140 cm^{-1}; $(PO_3OH)^{2-}$: δ (O_3PO) 350-580 cm^{-1}, γ POH 700-900 cm^{-1}, ν POH 860-915 cm^{-1}, ν_s PO_3 940-1010 cm^{-1}, ν_{as} 1040-1170 cm^{-1}, δ POH 1210-1400 cm^{-1}, and combination bands at 1400-1750 cm^{-1}), if they are Raman and/or infrared active [35].

Raman spectroscopy of dussertite

Because the complete Raman spectra of the dussertite minerals from Algeria and Germany are not provided, the spectra were only shown up to 1100 cm^{-1}. The complete infrared spectrum for dussertite from Krásno is given in Fig. S1. The results of the Raman and infrared spectral analysis are summarised in Table 1.

The Raman spectra of the mineral dussertite from three different localities in the 600 to 1000 cm^{-1} region are displayed in Fig. 1. In the spectral region from 700 to 950 cm^{-1} a complex set of overlapping bands is observed. For the Algerian dussertite four bands are inferred from the deconvolution analysis at 722, 794, 819, 859 and 893 cm^{-1}. According to Myneni *et al.* [28, 29], the proposed assignment of these bands is as follows: (a) the band at 893 cm^{-1} is assigned to the uncomplexed As-O_3 ν_3 antisymmetric stretching mode of the $(AsO_3OH)^{2-}$ polyhedron (b) the band at 859 cm^{-1} is assigned to the uncomplexed As-O_3 ν_1 symmetric stretching mode, due to its intensity (c) the band at 819 cm^{-1} is ascribed to As-OBa stretching mode (d) the band at 794 cm^{-1} is ascribed to the As-OFe ν_1 symmetric stretching mode (e) the band at 722 cm^{-1} is assigned to the complexed As-OH ν_1 symmetric stretching mode. The assignments of Ba- and Fe- stretching modes were derived based on different bond-lengths in highly-probable isostructural antimonian dussertite. But overlapping of the As-O$M^{2+/3+}$ bands with hydroxyl deformations is likely. For the German dussertite, Raman bands are observed at 808, 827, 864 and 896 cm^{-1}. The assignment of the bands is the same as

for the Algerian dussertite. The bands in the Raman spectrum of the Czech dussertite are broader. Raman bands are observed at 674, 724, 754, 825, 859, 870 and 902 cm^{-1}. The two high wavenumber bands at 870 and 902 cm^{-1} are assigned to the As-O ν_1 symmetric stretching mode and As-O ν_3 antisymmetric stretching mode of the uncomplexed As-O bonds. Bands at 859 and 825 cm^{-1} are attributed either to hydroxyl deformation modes or stretching As-O$M^{2+/3+}$ vibrations. The split band at ~700 cm^{-1} containing shoulders is ascribed to complexed As-OH symmetric and antisymmetric stretching vibration. On the basis of these assignments it is proposed that all the minerals studied contain variable amounts of protonated $(AsO_4)^{3-}$ groups in the $(AsO_3OH)^{2-}$ form. Variation in the spectra between the three dussertite mineral samples may be attributed to differences in composition. The infrared spectrum of Czech dussertite in the 650 to 1000 cm^{-1} region is shown in Fig. S2. The infrared spectrum compliments the Raman spectrum. Infrared bands are found at 810, 852, 881, 913 and 938 cm^{-1} as inferred from the deconvolution analysis. The infrared bands at 913 and 938 are assigned to the As-O ν_3 antisymmetric stretching mode and the band at 881 cm^{-1} to the As-O ν_1 symmetric stretching mode, which is active in the infrared spectrum. The bands at 852 and 810 cm^{-1} are assigned to the As-O$M^{2+/3+}$ stretching modes or hydroxyl deformation modes.

The Raman spectra of dussertite in the 100 to 600 cm^{-1} region are reported in Fig. 2. For the Algerian dussertite, Raman bands are observed at 358, 405, 462 and 471 cm^{-1}. The two bands at 358 and 405 cm^{-1} are attributed to the ν_2 $(AsO_4)^{3-}$ bending mode. The two high wavenumber bands are assigned to the ν_4 $(AsO_4)^{3-}$ bending mode. A similar set of bands may be found for the German dussertite. The two bands at 367 and 405 cm^{-1} are ascribed to the ν_2 $(AsO_4)^{3-}$ bending vibration and the single band at 471 cm^{-1} is assigned to the ν_4 $(AsO_4)^{3-}$ bending mode. For the Czech dussertite, Raman bands are observed at 372 and 409 cm^{-1}. These bands may be attributed to the ν_2 $(AsO_4)^{3-}$ bending vibration. The bands at 474 cm^{-1} and probably also at 429 cm^{-1} are designated to the ν_4 AsO_4^{3-} bending mode. In each of the spectra a band is observed in the 557 to 567 cm^{-1} region. This band is attributed to the ν_4 $(AsO_3OH)^{2-}$ bending mode. As for the $(AsO_4)^{3-}$ stretching region, there is a great deal of commonality between the three data sets despite the expected variation in composition. The ν_2 $(AsO_4)^{3-}$ bending vibration should be common to all hydroxyl arsenates, and should be relatively intense. Raman bands are observed at 350 cm^{-1} for olivenite, 340 cm^{-1} for cornwallite, and at 380 cm^{-1} for clinoclase [26].

Raman bands are observed in the far low wavenumber region in each of the spectra (Fig. 2). Three bands are observed at 208, 251 and 296 cm^{-1} (Algerian), 202, 252 and 296 cm^{-1} (German), and 247, 275 and 306 cm^{-1} (Czech). It is proposed that these bands are associated with Ba-O and Fe-O stretching vibrations. Intense bands at 188 cm^{-1} (Algerian), 191 cm^{-1} (German), and 188 cm^{-1} (Czech) are considered to be associated with the OH units and it is proposed that these bands are due to the hydrogen bonding of the OH units to the arsenate units.

The Raman spectrum of the Czech dussertite in the region 3300 to 3600 cm^{-1} is shown in Fig. 3. Raman bands are observed at 3015, 3242, 3371 and 3452 cm^{-1}. The first three bands are assigned to water adsorbed on the surface of the dussertite and/or coordinated water in the structure of dussertite. The last band at 3452 cm^{-1} is assigned to the stretching vibrations of the OH units. In the Raman spectrum of the Algerian dussertite, an intense Raman band at 3348 cm^{-1} is observed. Three broad bands for this dussertite sample are observed at 3023, 3222 and 3371 cm^{-1}. The observation of Raman (and infrared) bands in the 3015 to 3371 cm^{-1} shows water is strongly hydrogen bonded. This suggests that water molecules may be involved in the dussertite structure. The presence of molecular water in the crystal structure of dussertite is supported by the X-ray single-crystal study of antimonian dussertite published by Kolitsch *et al.* [1]. The presence of water in the structure may be necessary for the stability of the mineral.

The infrared spectrum of the Czech dussertite in the region 2800 to 3600 cm^{-1} is shown in Fig. S3. The infrared band at 3446 cm^{-1} is ascribed to the OH stretching vibrations of the hydroxyl units in the dussertite structure. This band is the equivalent of the Raman band observed at 3452 cm^{-1}. This band is sharp for bands in this spectral region, whereas water bands are quite broad. The broad band at 3223 cm^{-1} is assigned to hydrogen bonded OH groups and water molecules. Raman spectrum of dussertite in the region of the δ (ν_2) H_2O bending vibrations does not prove the presence of molecular water. However, in the infrared spectrum are observed bands at 1634 and probably also 1562 cm^{-1} which may be connected with these vibrations. The bands at 1384 and 1347 cm^{-1} may be related to the δ M/OH bending vibrations or overtones and/or combination bands. Raman bands at 1250, 1220, 1176 and 1115 are attributed to the δ As-OH and δ P-OH bending vibrations and ν_3 $(PO_4)^{3-}$ antisymmetric stretching vibrations. Some authors (see the Introduction) assume that dussertite may contain only hydroxyl ions, but according to other authors dussertite may

contain molecular water in its crystal structure, similarly as some other minerals of the crandallite group. Thus the question of this crystal-coordination of molecular water in the studied dussertite sample was not resolved on the basis of the Raman spectra but may be inferred from the infrared spectra studied in this paper.

CONCLUSIONS

The Raman spectrum of dussertite from the Huber stock deposit, Krásno near Horní Slavkov ore district, the Slavkovský les Mountains, Czech Republic was obtained and the spectrum compared with the Raman spectrum of dussertite downloaded from the RRUFF web site. The spectra showed great similarity as might be expected. Raman bands attributable to the stretching and bending vibrations of the $(AsO_4)^{3-}$ and $(AsO_3OH)^{2-}$ units are obtained. This suggests that dussertite contains OH^- group. The OH contents in dussertite should be variable. Some bands were assigned to the $(PO_4)^{3-}$ and $(PO_3OH)^{2-}$ vibrations.

The Raman spectrum shows a complex set of overlapping bands in the OH stretching region. Raman bands are observed at 3015, 3242, 3371 and 3452 cm^{-1}. The first three bands are assigned to water adsorbed on the surface of the dussertite and/or coordinated water in the structure of dussertite. The observation of Raman (and infrared) bands in the 3015 to 3371 cm^{-1} shows water is strongly hydrogen bonded. This suggests that water molecules are involved in the dussertite structure. The presence of molecular water in the crystal structure of dussertite is supported by the X-ray single-crystal study of antimonian dussertite published by Kolitsch *et al.* [1]. The presence of water in the structure may be necessary for the stability of the mineral. The infrared band of the OH stretching region is well defined. The broad infrared band of hydrogen bonded molecular water and/or hydroxyls centred upon 3223 cm^{-1} is observed together with two bands at 1634 and 1562 cm^{-1}, related to the H_2O bending vibrations. This broad band is not observed in the Raman spectrum.

Acknowledgements

The financial and infra-structure support of the Queensland University of Technology Inorganic Materials Research Program of the School of Physical and Chemical Sciences is gratefully acknowledged. The Australian Research Council (ARC) is thanked for funding the instrumentation. This work was financially supported by Ministry of Culture of the Czech

Republic (MK00002327201) to Jiří Sejkora and Jakub Plášil and by a long term Research Plan of the Ministry of Education of the Czech Republic (No. MSM0021620857) to Ivan Němec. The downloading of the Raman spectra of dussertite from the RRUFF web site is acknowledged.

309 **REFERENCES**

310 [1] U. Kolitsch, P. G. Slade, E. R. T. Tiekink, A. Pring, *Mineral. Mag.* **1999,** *63,* 17-26.

311 [2] J. W. Anthony, R. A. Bideaux, K. W. Bladh, M. C. Nichols, Handbook of

312 Mineralogy, Mineral Data Publishing, Tuscon, Arizona, USA, 2000.

313 [3] J. A. Mandarino, M. E. Back, Fleischer's Glossary of Mineral Species, The

314 Mineralogical Record Inc, Tucson, Arizona, U.S.A., 2004.

315 [4] K. Walenta, *Tschermaks Min. Petr. Mitt.* **1966,** *11,* 121-164.

316 [5] K. Walenta, *Die Mineralien des Schwarzwaldes und ihre Fundstellen, Weise*

317 *München* **1992**.

318 [6] A. N. Winchell, H. Winchell, Elements of Optical Mineralogy, Wiley, New York,

319 1951.

320 [7] M. Fleischer, R. E. Wilcox', J.J. Matzko, Microscopic Determination of the

321 Nonopaque Minerals, U. S. Geol. Survey Bull., Nedra Leningrad (in Russian), 1987.

322 [8] U. Kolitsch, P. G. Slade, E. R. T. Tiekink, A. Pring, *Min. Mag.* **1999,** *63,* 17-26.

323 [9] R. L. Frost, S. Bahfenne, *J. Raman Spectrosc.* **2009,** *40,* 360-365.

324 [10] R. L. Frost, S. Bahfenne, J. Graham, *J. Raman Spectrosc.* **2009,** *40,* 855-860.

325 [11] R. L. Frost, J. Cejka, *J. Raman Spectrosc.* **2009,** *40,* 591-594.

326 [12] R. L. Frost, J. Cejka, *J. Raman Spectrosc.* **2009,** *40,* 1096-1103.

327 [13] R. L. Frost, J. Cejka, M. J. Dickfos, *J. Raman Spectrosc.* **2009,** *40,* 355-359.

328 [14] R. L. Frost, J. Cejka, M. J. Dickfos, *J. Raman Spectrosc.* **2009,** *40,* 476-480.

329 [15] R. L. Frost, E. C. Keeffe, *J. Raman Spectrosc.* **2009,** *40,* 249-252.

330 [16] R. L. Frost, E. C. Keeffe, *J. Raman Spectrosc.* **2009,** *40,* 244-248.

331 [17] R. L. Frost, E. C. Keeffe, *J. Raman Spectrosc.* **2009,** *40,* 509-512.

332 [18] R. L. Frost, E. C. Keeffe, *J. Raman Spectrosc.* **2009,** *40,* 866-869.

333 [19] R. L. Frost, E. C. Keeffe, *J. Raman Spectrosc.* **2009,** *40,* 1117-1120.

[20] R. L. Frost, A. Soisnard, N. Voyer, S. J. Palmer, W. N. Martens, *J. Raman Spectrosc.* **2009,** *40,* 645-649.

[21] S. J. Palmer, R. L. Frost, H. J. Spratt, *J. Raman Spectrosc.* **2009,** *40,* 1138-1143.

[22] J. Sejkora, P. Ondrus, M. Fikar, F. Veselovsky, Z. Mach, A. Gabasova, R. Skoda, P. Beran, *J. Czech Geol. Soc.* **2006,** *51,* 57-101.

[23] K. M. Scott, *Am. Mineral.* **1987,** *72,* 178-187.

[24] V. Reppke, *Aufschluss* **1988,** *39,* 191-192.

[25] J. L. Jambor, J. Viñals, L. A. Groat, M. Raudsepp, *Can. Mineral.* **2002,** *40,* 725-732.

[26] W. N. Martens, R. L. Frost, J. T. Kloprogge, P. A. Williams, *Amer. Mineral.* **2003,** *88,* 501-508.

[27] T. Mihajlović, E. Libowitzky, H. Effenberger, *J. Solid State Chem.* **2004,** *177,* 3963-3970.

[28] S. C. B. Myneni, S. J. Traina, G. A. Waychunas, T. J. Logan, *Geochim. Cosmochim. Acta* **1998,** *62,* 3285-3300.

[29] S. C. B. Myneni, S. J. Traina, G. A. Waychunas, T. J. Logan, *Geochim. Cosmochim. Acta* **1998,** *62,* 3499-3514.

[30] K. Nakamoto, Infrared and Raman Spectra of Inorganic and Coordination Compounds, Wiley New York 1986.

[31] F. K. Vansant, B. J. V. D. Veken, *J. Mol. Struc.* **1973,** *15,* 439-444.

[32] F. K. Vansant, B. J. V. D. Veken, H. O. Desseyn, *J. Mol. Struct.* **1973,** 425-437.

[33] A. G. Nord, P. Kierkegaard, T. Stefanidis, J. Baran, *Chem. Commun. University Stockholm* **1988,** *5,* 1-40.

[34] P. Keller, *Neues Jb. Miner. Mh.* **1971,** 491-510.

[35] V. V. Pechkovskii, P. Y. Melnikova, E. D. Dzyuba, T. I. Baranikova, M. V. Nikanovich, Atlas of Infrared Spectra of Phosphates. Orthophosphates. Nauka (in Russian), Moscow 1981.

Dussertite Czech Raman	Dussertite Czech Infrared	Dussertite Algeria Raman	Dussertite Germany Raman	Suggested assignments
3452(s)	3446 (m)	3348 (s)		OH stretching vibrations
3439 (w)				OH stretching vibrations of the hydroxyl units
3371 (s)	3223 (m)	3371 (s)		OH stretching vibrations of hydrogen bonded water molecules and hydroxyls
3242 (s) 3015 (w) 1250 1220 1176 1115 (w)	3140 (w) 1634 (w) 1562 (w) 1384 (w) 1347 (w)	3222 (m) 3023 (w)		OH stretching vibrations of hydrogen bonded water molecules and hydroxyls δ H_2O bending δ M-OH bending vibration δ As-OH and δ P-OH bending, ν_3 $(PO_4)^{3-}$ antisymmetric stretching
	938			$(AsO_4)^{3-}$ ν_3 antisymmetric stretching
902 (s)	913	893	896	$(AsO_4)^{3-}$ ν_1 symmetric stretching
870 (s)	881	859	864	(AsO_4^{3-}) ν_1 symmetric stretching
859 (m)	852	819	827	As-O$M^{2+/3+}$ stretching and/or hydroxyl deformation
825 (w)	810	794	808	As-O$M^{2+/3+}$ stretching and/or hydroxyl deformation
754 (w)	752		721	ν As-OH stretching
724 (w)	702	722	707	ν As-OH stretching
561, 567 (m)		557	564	ν_4 $(AsO_3OH)^{2-}$ bending
474 (s)		471	471	ν_4 $(AsO_4)^{3-}$ bending
429 (s)		462		ν_4 $(AsO_4)^{3-}$ bending
409 (w)		405	405	ν_2 $(AsO_4)^{3-}$ bending
372 (w)		358	367	ν_2 $(AsO_4)^{3-}$ bending
306 (w)		296	296	Ba-O, Fe-O stretching
275 (s)		252	252	Ba-O, Fe-O stretching
247 (s)		202	202	Ba-O, Fe-O stretching
188 (m)		181	191	hydrogen bonding of the OH units to the arsenate

Table 1 Table of the Raman and infrared spectral results of dussertite from Algeria, German and Czech Republic [S=intense; m=medium intensity; w=low intensity]

List of Figs.

List of Tables

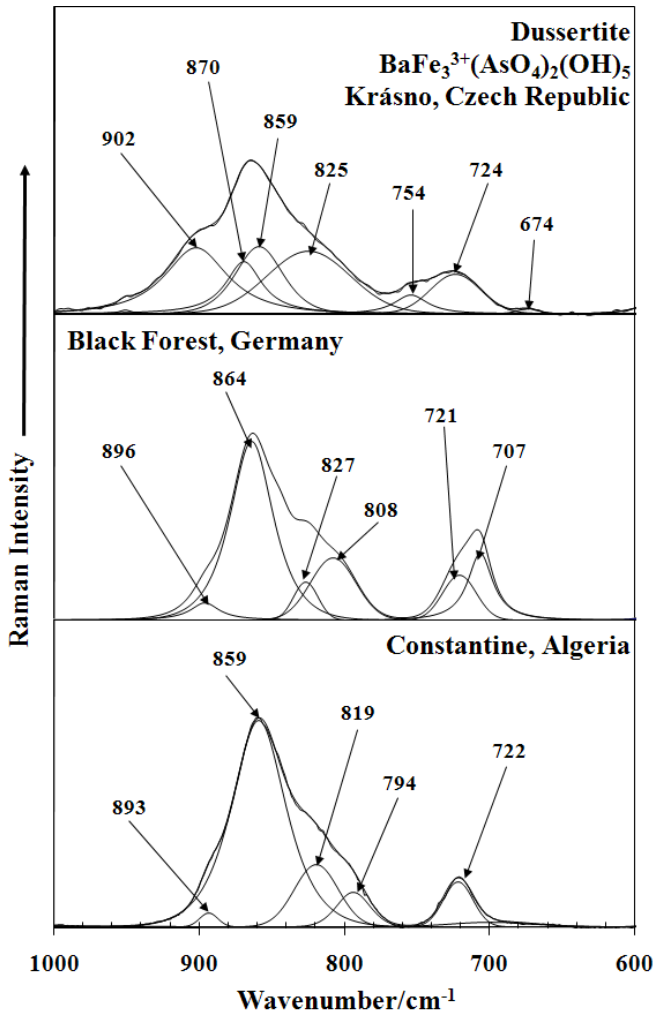

385
386 **Fig. 1**

387

388

389

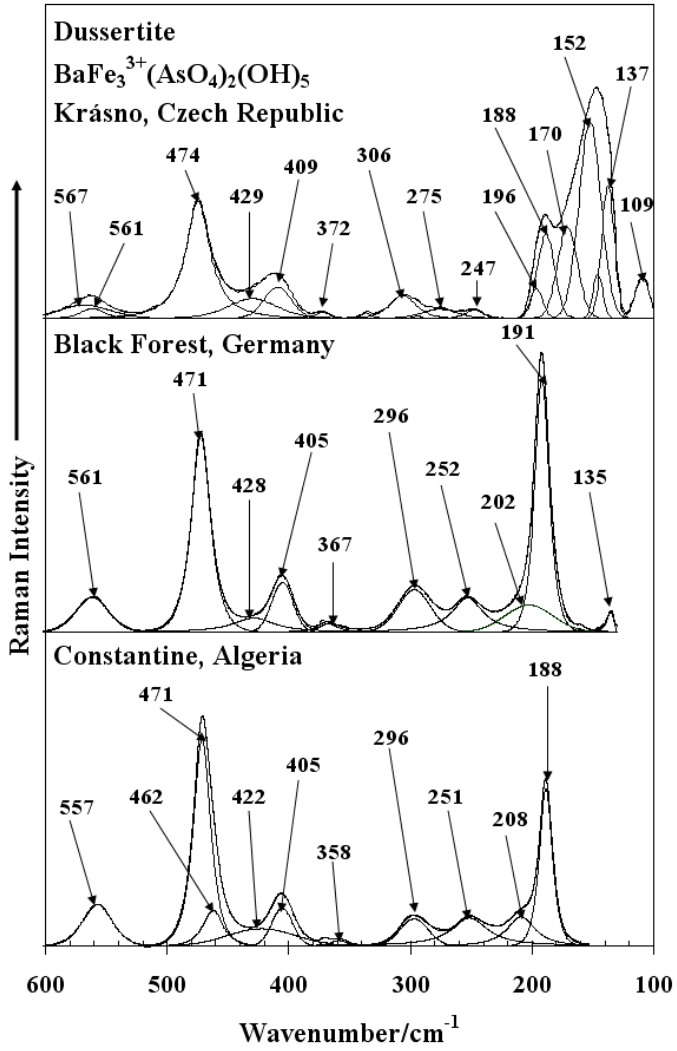

390

391

392 **Fig. 2**

393

394

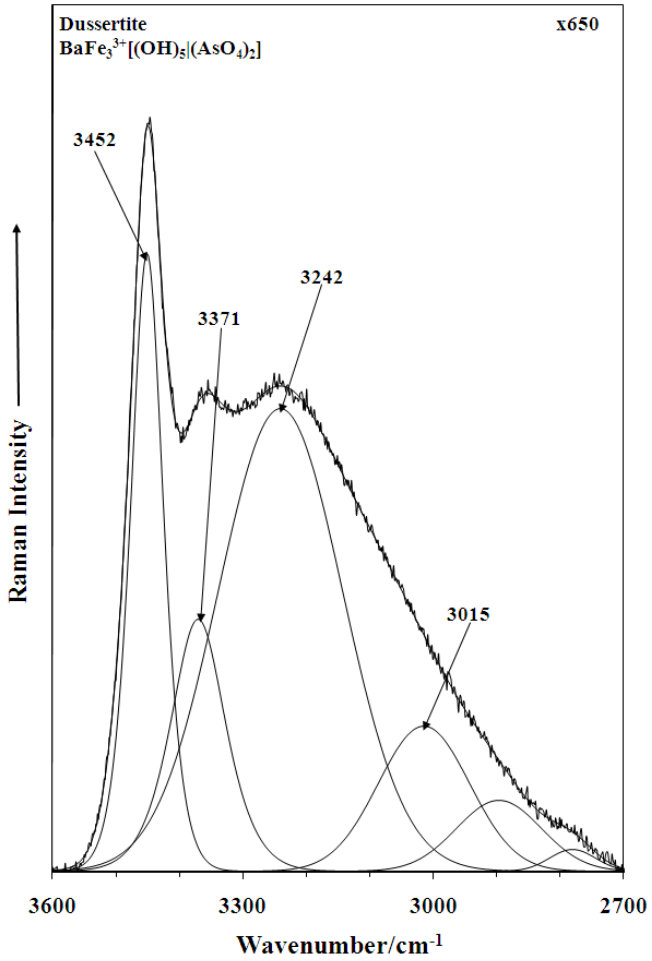

395

396

397 **Fig. 3**

398

399

400